PERGAMON

International Journal of Heat and Mass Transfer 43 (2000) 1851–1858

International Journal of HEAT and MASS TRANSFER

www.elsevier.com/locate/ijhmt

Optimization of a horizontal MOCVD reactor for uniform epitaxial layer growth

W.K. Cho, D.H. Choi*

Department of Mechanical Engineering, Korea Advanced Institute of Science and Technology, Taejon 305-701, South Korea

Received 9 April 1999; received in revised form 25 June 1999

Abstract

The numerical optimization scheme developed previously is successfully applied to optimize the geometric shape of a horizontal metal-organic chemical vapor deposition reactor for a uniform epitaxial layer of compound material. The procedure is based on sequential linear programming in which the reactor shape is approximated by the Chebyshev polynomials. A SIMPLE-type finite volume method is used on a general nonorthogonal grid to obtain the flow characteristics by solving the fully elliptic momentum, energy, and concentration equations. It has been demonstrated that more than a 30-fold improvement in uniformity can be achieved by this optimization for various flow and geometric conditions considered in this study. The optimization is also found effective for mixed convection flows as the buoyancy driven recirculation may be suppressed completely.

Keywords: MOVCD; Film uniformity; Optimal reactor shape; FVM; Reduced basis method

1. Introduction

Epitaxial layers, the geometric structure of which imitates that of the solid substrate, have important bearing on the performance of the electronic or opto-electronic devices. For instance, the compound semiconductors are largely made of the epitaxial-layer-coated wafer, and its yield depends very much on layer quality. Metal-organic chemical vapor deposition (MOCVD), which grows a solid film on the wafer surface from gas phase reactants through pyrolysis and chemical reaction, is one of the most popular techniques to make an epitaxial layer. The process is known to produce a layer which is generally uniform both in thickness and composition. However, for very demanding applications, needs to improve its quality to ever higher level have never diminished. Perhaps, the most critical element that determines the film quality is the thickness uniformity from the fluid-dynamics perspective as the growth rate in the mass-transfer-limited regime [1,2] is governed by the flow characteristics.

A horizontal reactor is superior to a vertical one in its productivity and therefore is preferred in industrial use. The uniformity of the film, however, is hampered by the reactant depletion due to the deposition process along the flow direction. Most of the work done on improving the quality of the film in a horizontal reactor is to make the cross-sectional area of the reactor vary in the streamwise direction. Gradual reduction of the cross-sectional area by tilting the susceptor or the top wall [3–6] helps as this accelerates the flow and effectively compensates the reactant depletion effects. The perfect uniformity may be achieved when these

* Corresponding author. Tel.: +82-42-869-3018; fax: +82-42-869-3210.

E-mail address: dhchoi@hanbit.kaist.ac.kr (D.H. Choi).

0017-9310/00/$ - see front matter
PII: S0017-9310(99)00251-3

two effects are exactly matched. Since the depletion is not linear in the streamwise direction, simple tilting of the planar wall would not be sufficient. Holstein [5] suggested that the film-thickness uniformity over a large surface area can only be achieved by forming a nonplanar susceptor or a top wall. As the curved susceptor is unthinkable, only choice we have is to make the top wall nonplanar.

The objective of this paper is to find an optimal shape of a horizontal reactor: representing the top-wall profile by a 4th-degree polynomial, the coefficients of which are determined to give the most uniform epitaxial layer possible. The procedure developed earlier [7,8] that finds the optimal inlet conditions for a vertical CVD reactor, has been modified and used for this purpose. The optimal shape has been obtained for various operating conditions, i.e. flow rates, buoyancy effects, etc., and the resulting film uniformity is found to be quite satisfactory for all cases examined. The discussions on the effects of the degree of basis function and the off-design point performance, which is very critical for this shape optimization to be truly practical, are also presented in the paper.

2. Analysis method

The flow in a horizontal reactor may be considered two-dimensional, if the reactor width is sufficiently large compared to the height, and remains laminar for most convenctional CVD operating conditions. For two-dimensional, laminar flows, the governing equations of continuity, momentum, energy and concentration, in nondimensionalized variables $\mathbf{u} = \mathbf{u}^*/u_{\text{in}}$, $x = x^*/h$, $y = y^*/h$, $T = (T^* - T_{\text{L}})/(T_{\text{H}} - T_{\text{L}})$ and $C = C^*/C_{\text{in}}$ are written as:

$$\nabla \cdot \mathbf{u} = 0, \tag{1}$$

$$\mathbf{u} \cdot \nabla \mathbf{u} = -\nabla p + \frac{1}{Re}\nabla^2 \mathbf{u} - \frac{Gr}{Re^2}\frac{\mathbf{g}}{|\mathbf{g}|}T, \tag{2}$$

$$\mathbf{u} \cdot \nabla T = \frac{1}{Re\ Pr}\nabla^2 T, \tag{3}$$

$$\mathbf{u} \cdot \nabla C = \frac{1}{Re\ Sc}\nabla^2 C, \tag{4}$$

where $\mathbf{u}$ is the velocity vector, p the hydrostatic pressure, T the temperature, and C the concentration of the rate-limiting species. The superscript * denotes the dimensional variable, the subscript in the inlet quantity and h the reactor height. The dimensionless parameters Re $(=u_{\text{in}}h/\nu)$, Pr $(=\nu/\alpha_{\text{T}})$, Sc $(=\nu/\alpha_{\text{M}})$, are Reynolds number, Prandtl number and Schmidt number, where

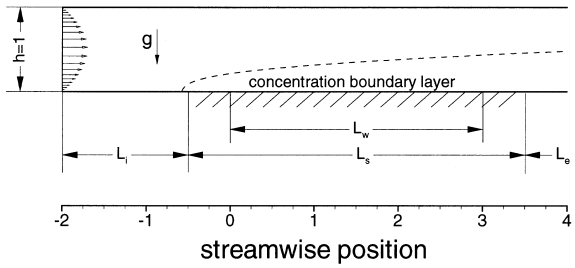

Fig. 1. Schematic of a horizontal reactor.

ν, α_{T}, α_{M} are the kinematic viscosity, the thermal diffusivity and the mass diffusivity, respectively. The temperature of the reacting surface is maintained to be T_{H} while that of the remaining surfaces is kept cold at T_{L}. The buoyancy is taken into consideration within the limits of incompressible flow; The Boussinesq approximation has been invoked to obtain the momentum equation in which the Grashof number Gr is given by $|\mathbf{g}|\beta(T_{\text{H}} - T_{\text{L}})h^3/\nu^2$. The effects of thermal diffusion on the growth rate are negligible in this flow regime and are ignored. A further justification for omitting the thermal diffusion effects may be found from the fact that our interest in this study lies primarily in the growth-rate uniformity, which is reported to be insensitive to the thermal diffusion even when the growth rate gets affected noticeably [6].

The schematic of a horizontal CVD reactor is shown in Fig. 1. The length of the substrate on which the deposition takes place is L_{s}. However, the wafers are placed on only part of that, i.e. L_{w} $(< L_{\text{s}})$ to avoid the definite discontinuity at both ends of the reacting surface where the growth rate reaches maximum or minimum [4]. The inlet/exit of the computational domain is placed at a distance $L_{\text{i}}/L_{\text{e}}$ upstream/downstream of the substrate.

The following boundary conditions for $\boldsymbol{u}$, T, and C are specified along the respective boundaries:

$$\text{inlet (given):} \quad u_x = 6u_{\text{in}}(1-y)y, \quad u_y = 0, \quad T = 0, \quad C = 1, \tag{5}$$

$$\text{exit:} \quad \frac{\partial u_x}{\partial x} = \frac{\partial u_y}{\partial x} = \frac{\partial T}{\partial x} = \frac{\partial C}{\partial x} = 0, \quad \frac{\partial p}{\partial x} = \text{const}, \tag{6}$$

$$\text{solid surface:} \quad u_x = u_y = \frac{\partial p}{\partial n} = 0, \quad T = 1, \quad C = 0 \text{ (substrate)}, \quad T = 0, \quad \frac{\partial C}{\partial n} = 0 \text{ (other surfaces)}. \tag{7}$$

The vanishing concentration on the substrate is due

to the deposition that accompanies chemical reaction [4–8].

Chemical deposition phenomena involve hundreds of reaction steps and chemical species. However, it suffices to consider only the group III containing species, e.g. $Ga(CH_3)_3$ (TMG, tri-methyl gallium) for GaAs epitaxial film growth, in the mass-transfer-limited regime [2]. Using the one-species model, the film growth rate is expressed by Fick's law as

$$G^* = \alpha_M \frac{\partial C^*}{\partial y^*} \frac{M_F}{\rho_F}, \tag{8}$$

where M_F is the molecular weight and ρ_F the density of the growing solid. The nondimensionalization by $G = G^*(h\rho_F/C_{in}\alpha_M M_F)$ results in $G = \partial C/\partial y$ in that the growth rate is identical to the normal concentration gradient on the substrate.

The SIMPLE-based finite volume method developed earlier for axisymetric flows [8] is extended to solve the governing equations. The reactor shape being optimized is fitted by a colocated nonorthogonal general grid. The diffusive derivatives in the equations are discretized by the central differencing while the convective derivatives are done by QUICK scheme [9] to preserve second-order accuracy. The process is iterative and the solution is considered to have converged when the sum of the residual over the entire domain in each equation becomes less than 10^{-5}.

3. Optimization technique

The cost function, a measure of the spatial nonuniformity of the growth rate on wafers, is defined as:

$$E = \left\{ \int_{A_w} (G - \bar{G})^2 \, dA/\bar{G}^2 A_w \right\}^{1/2}, \tag{9}$$

where $\bar{G}$ is the average growth rate and A_w is the area on which wafers are distributed.

The segment of the top wall to be modified is represented by a linear combination of Chebyshev polynomials $\varphi(x)$ as:

$$h(x) = \sum_{k=0}^{N} a_k \varphi_k(x) \tag{10}$$

where $h(x)$ represents the height at x and N the number of the basis functions; the task becomes to find the set of coefficients a_k that minimizes the cost function E. This approach, called reduced basis method [10], is efficient in finding an approximate optimal state and thus is widely used in many engineering applications, e.g. designing an optimal airfoil [11].

The procedure to determine a_k that gives minimum E could be time-consuming as the link between the two is highly nonlinear Navier–Stokes equations. An efficient scheme is laid out in Cho et al. [8] and a brief description is given below:

The growth rate $G(\mathbf{a})$ near $\mathbf{a}^0$ may be written as

$$G(\mathbf{a}) \approx G(\mathbf{a}^0) + \frac{\partial G}{\partial \mathbf{a}} \cdot \delta \mathbf{a}, \tag{11}$$

where $\mathbf{a} = \mathbf{a}^0 + \delta \mathbf{a}$. Using the random search technique [10], $\delta \mathbf{a}$ is sought to make E minimum within the specified move limit. The region inside the move limit is where Eq. (11) warrants sufficient accuracy. Once the move limit is reached, new flow analysis for each a_k is performed to obtain $\partial G/\partial a_k$ and the process continues. Although an additional integration of Eq. (9) is involved, which would have been omitted if the Taylor expansion (11) is used directly for E, the route described above was found to be more efficient [8], since G reflects the flow field better than E and thus a larger move limit can be taken.

The optimal state is considered reached when the relative variation of the cost function becomes less than 10^{-3}. The computation time may be greatly reduced if the optimal profile of the first degree is obtained first and used as an initial condition. Approximately 10–15 iterations, each of which consists of 5 flow analyses, are needed to arrive at the final shape. The whole process takes about 4.5 h on a 233 MHz Pentium PC for $Re = 40$.

4. Results and discussions

Before tackling the optimization problem, the flow solver is verified against the measured data [12] taken from a horizontal reactor of constant cross-section. The epitaxial film growth rate along the substrate obtained with a nonuniformly distributed 110×40 grid is compared in Fig. 2. The excellent agreement seen in Fig. 2 confirms that the code accurately predicts the epitaxial growth rate and is fit to be used in the present optimization process.

Owing to Fotiadis et al. [13], Pr and Sc for H_2 and $Ga(CH_3)_3$ as the working fluid (carrier gas) and the reactant gas at 900 K and 0.1 atm come out to be 0.7 and 2.33 since $\nu = 7 \times 10^{-3}$, $\alpha_T = 1 \times 10^{-2}$ and $\alpha_M = 3 \times 10^{-3}$ m^2/s. A thorough grid dependency test proves that a nonuniformly distributed 100×40 grid adequately resolves the flow field. Fig. 3 presents a typical grid; it should be noted that a new grid is generated every time when the shape has been modified. It is also verified that enlarging the computational domain or tightening the convergence criterion made little difference in growth rate distribution.

Various cases for different Reynolds numbers, ther-

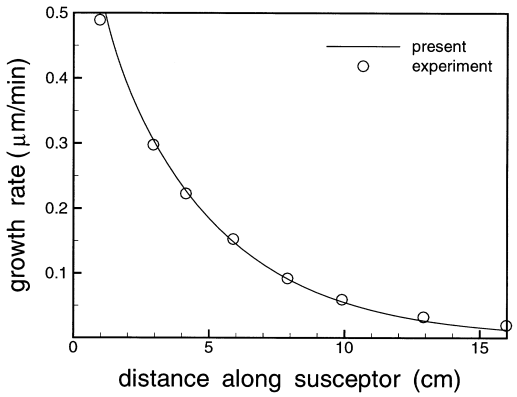

Fig. 2. Growth-rate distribution along the susceptor.

Table 1
Cost function and growth rate for various operating conditions

L_w	Re	Gr/Re^2	E (×100)		$\bar{G}$	
			UN[a]	OP[b]	UN[a]	OP[b]
3	10	0	20.8	0.386	2.07	4.49
3	20	0	19.8	0.335	2.69	5.84
3	40	0	19.3	0.321	3.47	7.72
3	10	30	31.9	0.757	2.17	4.58
3	10	40	34.5	0.886	2.24	4.61
3	10	50	36.4	1.01	2.31	4.64
6	40	0	25.2	0.910	2.92	6.56

[a] Unoptimized.
[b] Optimized.

mal conditions, and substrate lengths examined in the present study are summarized in Table 1. The resulting cost function and the mean growth rate are also tabulated for both before and after optimization; we will get back to this later in the paper. The first series of calculations is performed for the computational domain that extends from $x=-2$ to 6 with $L_s=4$ ($-0.5 \le x \le 3.5$) and $L_w=3$ ($0 \le x \le 3$). The length and the position of the top-wall segment that is being optimized are aligned with those of the substrate on the floor. The reactor height beyond the end of this segment is constant to the exit and comes out as part of the solution.

Fig. 4 shows the concentration fields for Re = 40 before and after the shape optimization. It is seen from the figure that the concentration boundary layer thickens rapidly for an unoptimized reactor while it remains much the same for the optimized one. The thickening concentration layer makes the deposition rate drop off rather quickly as illustrated in Fig. 5, whereas the right amount of flow acceleration due to the cross-sectional area reduction for the optimal reactor keeps the layer and thus the growth rate fairly constant along the substrate. An almost perfect uniformity is seen to be realized by modifying the reactor shape. The result for the reactor, whose top wall is tilted by an optimal angle, is also compared in Fig. 5. Although the improvement gained is substantial, it is far from being uniform as pointed out in Holsteins et al. [5]. Calculations for the unoptimized shape were repeated with coarser (76 × 33) and finer (156 × 56) grids, and the results are plotted together in Fig. 5. No discernable difference among the three is noticed and it confirms that the present grid is sufficiently fine to resolve the flow field accurately.

The cost function given in Table 1 demonstrates that about a 40-fold improvement in uniformity has been achieved for all three Reynolds number cases tested. It is also important to note that the Reynolds number effects on uniformity are not significant and the deposition efficiency too is improved by this optimization as the mean growth rate $\bar{G}$ is more than doubled after the shape has been modified.

The optimal reactor shapes for different Reynolds number cases are presented in Fig. 6. The general slope of the top wall is steeper for Re = 10 than for the other higher Re cases to compensate for the adverse diffusion effects: stronger diffusion enhances deposition earlier on and leaves less reactant gas for downstream use. It is important to note that the optimal shape remains unchanged when going from Re 20 to 40. To put this in better perspective, off-design-

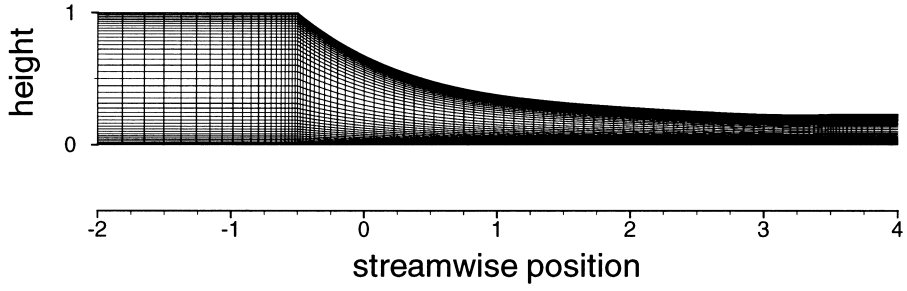

Fig. 3. Typical computational grid (110 × 40).

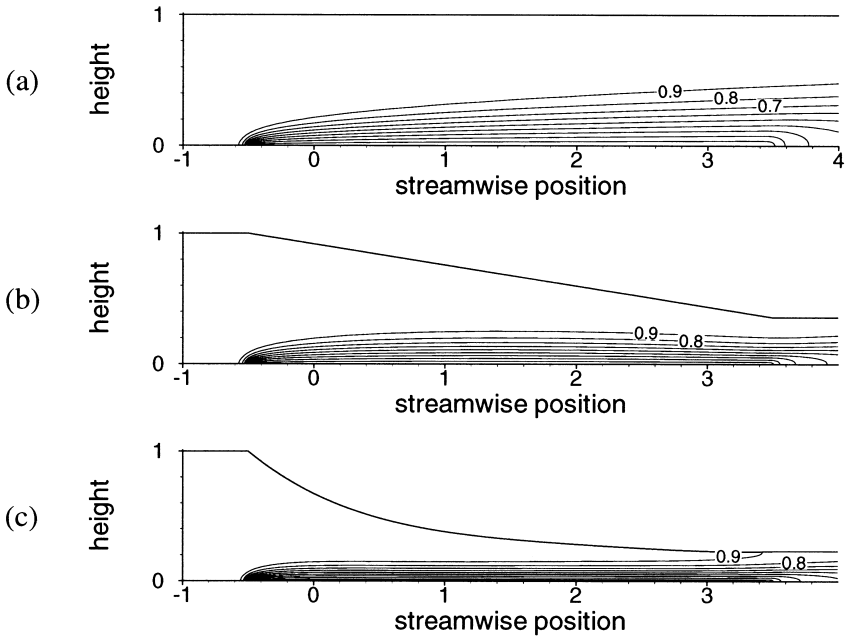

Fig. 4. Concentration fields for $Re = 40$. (a) Unoptimized; (b) optimized (linear function); (c) optimized (4th-degree polynomial).

point performance of the optimal reactor for $Re = 40$ is examined for $10 \leq Re \leq 100$. The cost function given in Table 2 exhibits that more than ten-fold improvement in uniformity over the unoptimized reactor is still achieved for $Re \geq 20$. Even when $Re = 10$, which is the worst case among the tested, the uniformity is improved about three times. This is very encouraging since a reactor, which is designed for one specific condition, is effective for a wide range of flow rates and makes the shape optimization even more practical. Less than 2% deviation in uniformity for $20 \leq Re \leq 100$ is quite remarkable considering that the cost function of a film grown in a planar top wall reactor with optimal tilt angle is of an order of 5% (see Table 3 or Ref. [5]).

Table 2
Off-design-point performance of the optimal reactor for $Re = 40$: E ($\times 100$)

Re	10	20	40[a]	100
Optimal reactor for $Re = 40$	7.96	1.17	0.321	1.46
Unoptimized reactor	20.8	19.8	19.3	18.9

[a] Design point.

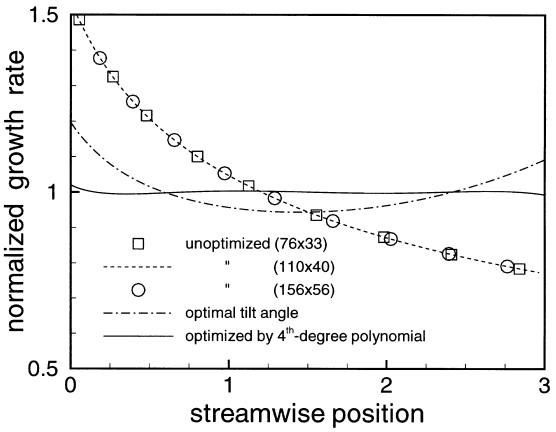

Fig. 5. Growth-rate distributions with and without optimization.

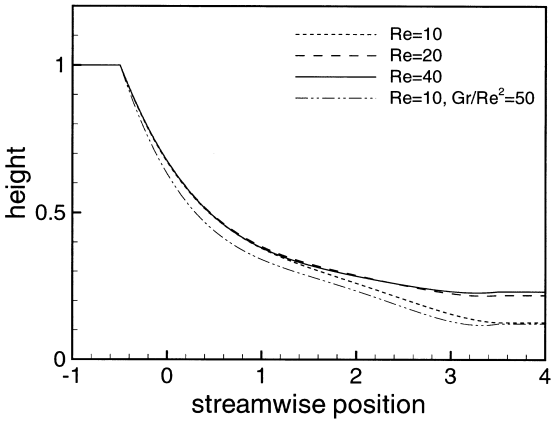

Fig. 6. Optimal reactor shapes for various flow conditions.

Table 3
Cost function vs. the number of basis functions for $Re = 40$

N	0	1	2	3	4	5
E ($\times 100$)	19.3	5.65	2.00	0.776	0.321	0.145

To check the completeness of the basis function, the number of the basis functions, N in Eq. (10), is varied from 0 to 5: $N = 0$ signifies the unoptimized reactor whereas $N = 5$ means that the top wall is approximated by a 5th-degree polynomial. Table 3 compares the cost function for these cases at $Re = 40$. It is safe to conclude from the table that the 3rd- or 4th-degree polynomial is adequate to approximate the profile as the additional gain obtained when using a higher-degree polynomial is not significant. Of course, one can readily go to a higher-degree polynomial whenever it becomes necessary.

A large temperature difference commonly exists in the flow field due to uneven heating for spatially selective deposition. This induces secondary flow and, as the convection parameter Gr/Re^2 increases, the potentially detrimental (to the deposition process) recirculation region(s) may develop [14]. The flow characteristics for $Re = 10$ and $Gr/Re^2 = 50$ in an unoptimized reactor are depicted in Fig. 7. Two separation bubbles (vortices) are seen to form along the reactor walls near both ends of the substrate (Fig. 7a), where the wall temperature goes up or down discontinuously. The front bubble pushes the flow downward while the rear one does the opposite; as a results, the concentration layer becomes thinner/thicker in the upstream/downstream region than would be without these effects as is presented in Fig. 7c. The growth rate shown in Fig. 8 exhibits the trend that the uniformity deteriorates further as Gr/Re^2 increases. However, after the shape has been optimized, the growth rate becomes quite uniform regardless of Gr/Re^2 as plotted in the figure (also in Table 1). Fig. 9 presents the optimal shape and corresponding flow characteristics for $Re = 10$ and $Gr/Re^2 = 50$: the vortices have disappeared completely, and the temperature and the concentration fields look pretty much evenly stratified.

As pointed out earlier in this paper, one important reason for using the reactor of horizontal type is its high throughput. Obviously, it is advantageous to make the reactor as long as possible. To check whether the optimization can be as effective for a longer substrate, we doubled L_w ($0 \le x \le 6.0$) and repeated the analysis for $Re = 40$. The computational domain and L_s were increased accordingly. The resulting reactor shape and the growth-rate distribution are shown in Fig. 10. The uniformity is still very satisfactory: it is a little wigglier than that of the shorter reactor presumably due to the single polynomial approximation of the longer top wall segment. The mean growth rate is

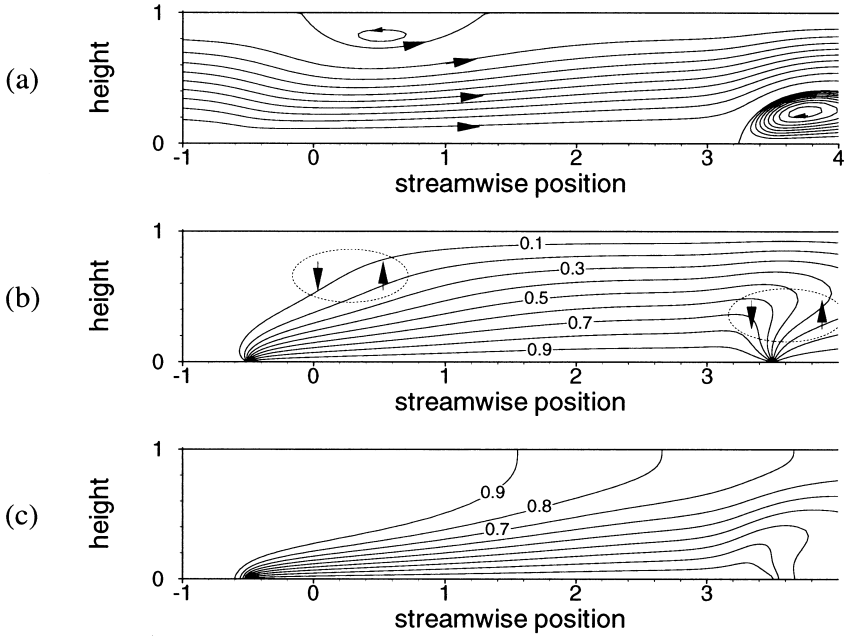

Fig. 7. Characteristics of mixed convection flow ($Gr/Re^2 = 50$) in an unoptimized reactor. (a) Streamlines; (b) temperature field; (c) concentration field.

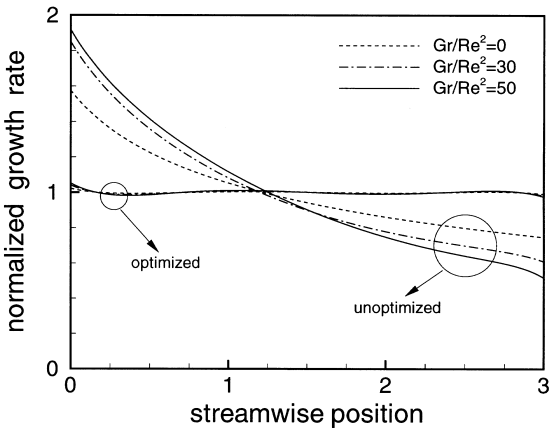

Fig. 8. Growth-rate distributions for varying degree of buoyancy effects.

about 15% less than that of the shorter reactor (see Table 1) and the flow rate must be increased to obtain the comparable growth rate. The fact is that the optimization works even for this length. It poses an interesting new problem that the optimal length should exist and how it can be determined. No attempt has been made in this regard including what a plausible cost function would be.

Finally, we examined how good the starting position of the top-wall segment being modified. We varied the points from −0.7 to −0.3, and the cost function distribution is presented in Fig. 11 for various Reynolds numbers. The position that yields the smallest cost function is indicated by the solid circle and appears to be very close to the reference point −0.5. This, together with the observation that the cost function does not vary rapidly in that neighborhood, suggests that the present choice of the starting location is adequate. The downstream movement of this optimal position for $Re = 10$ may be explained by the more active deposition due to the stronger diffusion effects. By delaying the starting point, the effect is lessened and the uniformity is improved.

5. Conclusions

An optimal shape for the horizontal reactor, is successfully obtained by the optimization scheme developed in this study. The 4th-degree polynomial that approximates the top-wall profile is determined to produce the most uniform epitaxial layer possible. A series of calculations has been carried out for various *Re*, *Gr* combinations, and for different substrate lengths. The results for all the cases tested are quite remarkable and satisfactory: The modified shape is seen to suppress the buoyancy driven recirculation effectively and some 30-fold improvement in uniformity has been achieved. The fact that the shape dose not change much for a

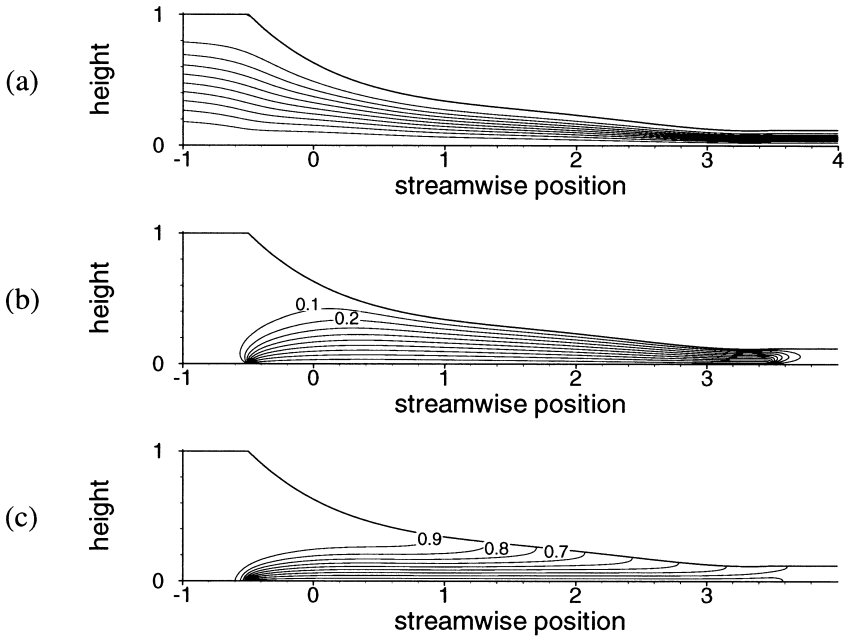

Fig. 9. Characteristics of mixed convection flow ($Gr/Re^2 = 50$) in an optimal shape reactor. (a) Streamlines; (b) temperature field; (c) concentration field.

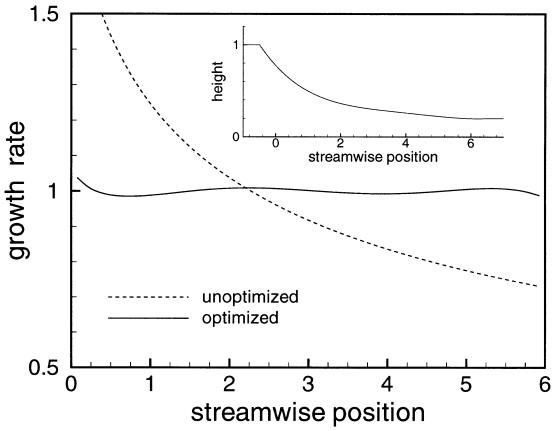

Fig. 10. Growth-rate distribution for $L_w = 6$ at $Re = 40$. Inset shows the optimal reactor shape.

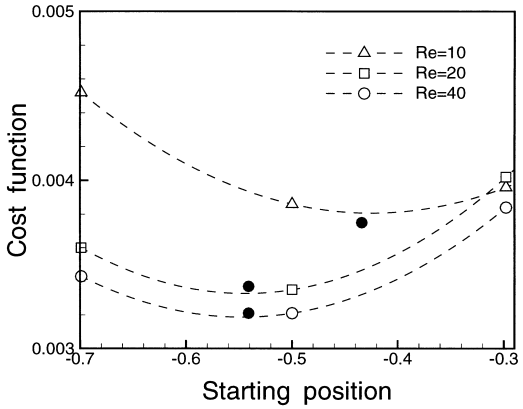

Fig. 11. Cost function vs. the starting position of the top-wall curve.

wide range of Reynolds numbers is also very encouraging as it makes the present optimization concept economically feasible.

References

[1] K.F. Jensen, Transport phenomena in vapor phase epitaxy reactors, in: D.J.T. Hurl (Ed.), Handbook of Crystal Growth, vol. 3b, Elsevier Science, Amsterdam, 1994, pp. 541–599.

[2] G.B. Stringfellow, A critical appraisal of growth mechanism in MOVPE, J. Crystal Growth 68 (1984) 111–122.

[3] K. Chen, Heat and mass transfer in horizontal vapor phase epitaxy reactors, J. Crystal Growth 70 (1984) 64–72.

[4] A.B. Bulsari, M.E. Orazem, J.G. Rice, The influence of axial diffusion on convective heat and mass transfer in a horizontal CVD reactors, J. Crystal Growth 92 (1/2) (1988) 294–310.

[5] W.L. Holstein, J.L. Fitzjohn, E.J. Fahy, P.W. Gilmour, E.R. Schmelzer, Mathematical modeling of cold-wall channel CVD reactors, J. Crystal Growth 94 (1) (1989) 131–144.

[6] A.N. Jansen, M.E. Orazem, B.A. Fox, W.A. Jesser, Numerical study of the influence of reactor design on MOCVD with a comparison to experimental data, J. Crystal Growth 112 (2/3) (1991) 316–336.

[7] W.K. Cho, D.H. Choi, M.U. Kim, Optimization of inlet concentration profile for uniform deposition in a cylindrical CVD chamber, Int. J. Heat Mass Transfer 42 (6) (1999) 1141–1146.

[8] W.K. Cho, D.H. Choi, M.U. Kim, Optimization of the inlet velocity profile for uniform epitaxial growth in a vertical MOCVD reactor, Int. J. Heat Mass Transfer 42 (22) (1999) 4143–4152.

[9] B.P. Leonard, A stable and accurate convective modelling procedure based on quadratic upstream interpolation, Comput. Meth. Appl. Mech. Eng. 19 (1) (1979) 59–98.

[10] G.N. Vanderplaats, Numerical Optimization Techniques for Engineering Design, McGraw-Hill, New York, 1984.

[11] S. Eyi, J.O. Hager, K.D. Lee, Airfoil design optimization using the Navier–Stokes equations, J. Opt. Theor. Appl. 83 (3) (1994) 447–461.

[12] J. Van de Ven, G.M.J. Rutten, M.J. Raaijmakers, L.J. Giling, Gas phase depletion and flow dynamics in horizontal MOCVD reactors, J. Crystal Growth 76 (2) (1986) 352–372.

[13] D.I. Fotiadis, S. Kieda, K.J. Jensen, Transport phenomena in vertical reactors for metal-organic vapor phase epitaxy: effects of heat transfer characteristics, reactor geometry, and operating conditions, J. Crystal Growth 102 (3) (1990) 441–470.

[14] E.P. Visser, C.R. Kleijn, C.A.M. Govers, C.J. Hoogendoorn, Return flows in horizontal MOCVD reactors studied with the use of TiO_2 particle injection and numerical calculations, J. Crystal Growth 94 (4) (1989) 929–946.